**Environmental Resources Research**
Vol. 6, No. 2, 2018

GUASNR

# Water erosion prediction using Revised Universal Soil Loss Equation and GIS: A case study of Gorganrud Basin

**S. Abedian[1*], A. Salmanmahiny[2]**
[1]Ph.D student of Environmental Sciences and Instructor of University, Department of Agriculture and Natural Resources, University of Payam-e-noor, Kerman, Iran.
[2] Professor of Environmental Sciences, Department of Environmental Sciences, Gorgan University of Agricultural Science and Natural Resources, Gorgan, Iran.

*Received: June 2017 ; Accepted: August 2018*

**Abstract**
Soil erosion and sedimentation processes can be considered as serious eco-environmental problems. This study aimed to estimate the basin-wide erosion using the Revised Universal Soil Loss Equation (RUSLE). The soil erosion parameters included rainfall erosivity map generated from the rainfall data, soil erodibility extracted from the soil map, land cover and management map produced from supervised classification of Landsat ETM+ data, and a Digital Elevation Model (DEM) to generate the slope length and steepness factor (LS) maps. Support practice map was assumed as 1 as there were no significant conservation practices. Then, the six thematic layers were integrated based on RUSLE model in GIS environment, and the spatial distribution of soil loss in the Gorganrud Basin was achieved. The distribution of erosion risk was 42.5% for low, 30.33% for moderate, and 27.17% for severe classes. The highest amount of erosion occurred in the northwest to northeast and eastern regions with lithological units including loess, young terraces and alluvial deposits and agricultural use despite the fact that LS factors in these areas were less than 10. In the central and southern parts of the basin, in spite of the high values of LS factor (15–55), these areas depicted low to moderate erosion potential. This is supposed to be due to the dense forest coverage in the region that decreases the energy of rain droplets. The soil erosion risk map can be used for rapid assessment of the effects of environmental changes and watershed management interventions.

***Keywords*:** Soil erosion, Erosion risk, watershed management, RUSLE.

* Corresponding author; sahar.abedian1985@gmail.com

## Introduction

Shifting cultivation in the hill slopes, neglect of soil conservation techniques and over exploitation of land or crop production due to population stress, lead to enormous soil erosion (Devatha *et al.*, 2015). The total land area subjected to human-induced soil degradation is estimated at about 2 billion hectares in the world. Saha (2003) estimated that the land area affected by soil degradation due to the erosion to be 1100 Mha by water erosion and 550 Mha by wind erosion in the world. Soil erosion by water is a major factor in land degradation process and has been accepted as an obstacle in the way of sustainable development of agriculture and natural resources in our modern time. The adverse influences of widespread soil erosion include sedimentation in rivers and reservoirs which can lead to eutrophication, siltation, and reducing lifetime of reservoirs; transfer of contaminants such as nutrients, pesticides, and toxic metals which could lead to downgrading of water quality. Moreover, it can change the water holding capacity and soil properties (Dorren *et al.*, 2004; Pathaka, 2005; Ganasri *et al.*, 2016; Devatha *et al.*, 2015; Arriaga and Lowery, 2003).

Soil erosion in Iran has a major effect on the quality and quantity of agricultural products, siltation of reservoirs, destructive floods, land degradation, etc. United Nation's Development Program has reported that the soil erosion in Iran is about 20 tons/ha, which has increased by 10 tons/ha compared to the last decade (UNDP, 1999). Overgrazing by livestock, unsustainable agricultural practices, over cropping and deforestation, commercial and industrial development, urban expansion, and road construction are the possible causes that accelerate the removal of soil material (Safamanesh *et al.*, 2006; Kheyrodin, 2016), which give rise to serious environmental problems and disastrous economic consequences. So, estimation of soil erosion potential and identification of critical soil loss-prone areas is necessary for best soil conservation management.

A wide range of models have been developed for erosion and sediment transport evaluation which differ in terms of complexity, processes considered, and data required for model calibration and model use (Ranzi *et al.*, 2012). Normally, it is a hard task to find a model that assesses all the contributing factors to erosion; however, some models have specifically been formulated to help conservation planners in erosion prone zoning and erosion management. One of the most widely used erosion models for estimating long-term average annual soil loss is the Universal Soil Loss Equation (USLE), introduced by Wischmeier and Smith in 1965 (Ganasri and Ramesh, 2016; Panagos *et al.*, 2015; Wischmeier and Smith, 1978; Renard *et al.*, 1997). It is an empirical quantitative model that predicts the long-term average annual rate of erosion based on rainfall erosivity, soil erodibility, slope length and steepness, cover management, and support practice (Kouli *et al.*, 2009; Renard *et al.*, 1997). RUSLE has the same formula as USLE, but with several improvements in determining factors. These include some new and revised isoerodent maps; a time varying approach for soil erodibility factor; a sub factor approach for evaluating the cover management factor; a new equation to reflect slope length and steepness; and new conservation practice values (Renard, *et al.*, 1997). Details for the calculation of RUSLE are given in Agriculture Handbook (No. 703) published by the U.S. Department of Agriculture.

Also, due to lack of sediment gauging station, limitation in implementation cost and time, it is necessary to integrate remote sensing and Geographic Information Systems (GIS) in soil erosion models. Considering the above aspects, the objectives of the present study was to apply the RUSLE model in GIS environment to estimate the total annual sediment yield in Gorganrud Basin, north of Iran. By using erosion models, we will be able to identify critical soil loss-prone areas and then prioritize them for soil conservation programs.

## Model Descriptions

The Revised Universal Soil Loss Equation (RUSLE) (Renard *et al.*, 1997) is a developed version of the Universal Soil Loss Equation, USLE (Wischmeier and Smith, 1978). RUSLE model enables the prediction of average annual rate of soil erosion for a site of interest for any number of scenarios involving cropping systems, management techniques, and erosion control practices (Kouli *et al.*, 2009). Six major factors (rainfall erosivity, soil erodibility, slope length and steepness, cover management, and support practice) are used in RUSLE method to compute the expected average annual erosion through Equation (1) (Renard *et al.*, 1997):

$$A = R \times K \times L \times S \times C \times P$$

Where $A$ is the computed spatial average soil loss and temporal average soil loss per unit area (ton /ha $yr^{-1}$), $R$ indicates the rainfall runoff erosive factor [MJ mm $ha^{-1}$ $h^{-1}yr^{-1}$], $K$ is the soil erodibility factor [ton ha h / (ha MJ mm)], $L$ is the slope length factor, $S$ is the slope steepness factor, $C$ is the cover management factor, and $P$ is the conservation support practice factor. $L$, $S$, $C$, and $P$ are all dimensionless. In this study, the soil erosion risk is classified into four levels according to Table 1 (Farhan, 2013; Li and Luo, 2006).

**Table 1.** Soil erosion risk level and intensity

| Erosion and torrent category | Qualitative name of erosion category | Rate of soil loss ($t/h^{-1}$ $yr^{-1}$) |
|---|---|---|
| I | Very low | 0-5 |
| II | Low | 5-15 |
| III | Moderate | 15-25 |
| IV | Severe | > 25 |

## Materials and methods

### Study area

The study area is situated in Golestan Province, south of Caspian Sea in Iran. The area of Gorganrud drainage basin is 1480 $Km^2$, which is located between latitudes 36° 30′-38° 8′ N and longitudes 53° 57′-56° 22′ E. The geomorphology of the study site is characterized by flat areas in the north and mountains in the south with elevations ranging from -23 to 3708 m (The Management and Planning Organization, 2007). The mean annual precipitation and temperature are 549 mm and 16 °C, respectively, which classify the site as Mediterranean based on Koppen (*Csa*) and De Martonne ($I$=21.6) methods. The main lithological units are shale, marl, limestone, dolomite, sandstone, and fluvial deposits in the study basin. To study land degradation in the study area, the basin was subdivided into homogeneous terrain units based on Digital Elevation Model (DEM) and river layer using Archydro Plus extension of ArcGIS software. Sub-basin characteristics are shown in Figure 1 and Table 2.

**Table 2.** Characteristics of sub-basins at the study area.

| Sub-basin | Length (Km) | Area ($Km^2$) | Average Slope (%) | Annual Temperature (°C) | Annual Precipitation (mm) |
|---|---|---|---|---|---|
| 1 | 24 | 151.74 | 16.07 | 15.1 | 605.76 |
| 2 | 18 | 115.90 | 13.88 | 17.2 | 542.08 |
| 3 | 16 | 90.55 | 36.78 | 16.3 | 640.41 |
| 4 | 18 | 65.79 | 16.25 | 15.7 | 652.29 |
| 5 | 17 | 151.98 | 9.61 | 14.7 | 640.39 |
| 6 | 24 | 144.71 | 18.40 | 14.8 | 642.06 |
| 7 | 16 | 250.55 | 45.35 | 8.9 | 524.71 |
| 8 | 11 | 141.84 | 27.21 | 6.5 | 370.22 |
| 9 | 13 | 133.89 | 34.09 | 5.3 | 399.85 |
| 10 | 14 | 93.81 | 32.20 | 9.2 | 564.05 |
| 11 | 33 | 139.22 | 34.32 | 10.2 | 464.51 |

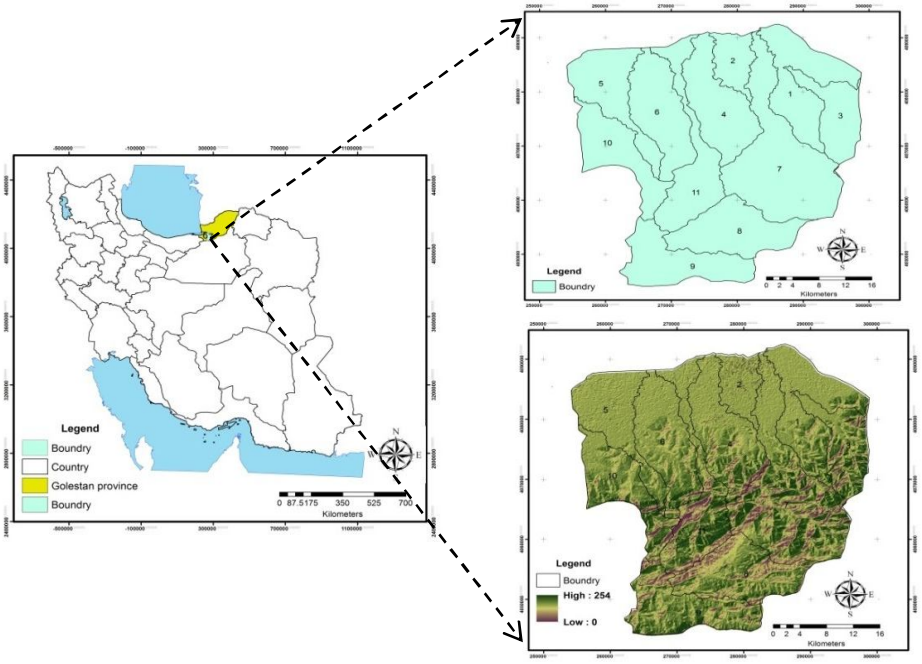


**Figure 1.** Geographical location of the Gorganrud Basin, Golestan Province, Iran.

**Data processing and RUSLE factors generation**

The RUSLE model was developed based on spatially distributed input data such as rainfall erosivity, soil erodibility, slope length and steepness, cover management, and support practice in a Geographic Information System environment for the calculation of annual soil loss. In the present study, the meteorological data for calculation of rainfall erosivity factor was derived from the Meteorological Organization. This tabular data was imported into ArcGIS as a point layer. In next stage, the Inverse Distance Weighted (IDW) spatial interpolation technique was used to generate raster maps for these parameters. Also, Landsat-ETM$^+$ satellite image was downloaded from earth explorer site and was used for producing and assessment of vegetation parameters in the area. Moreover, the LS factor was generated using Digital Elevation Model (DEM) with a resolution of 30 m through Raster Surface and Archydro Plus tools in ArcGIS. The DEM layer was provided by National Cartographic Center of Iran (NCC). The soil characteristic layer for calculation of soil erodibility factor was obtained from the Soil Geographic Data Base of Iran. This layer was reclassified based on soil particle size, organic matter content, soil structure, and profile permeability according to Wischmeier and Smith nomograph (1978). The cell size of all data layers was set at 30 m×30 m. In next stage, the layers were overlaid and multiplied pixel by pixel, using Equation 1 to determine the spatial average soil loss per unit area.

**Soil erodibility factor (K)**

The Soil erodibility factor represents both susceptibility of soil to erosion and the amount and rate of runoff (Devatha *et al.*, 2015). The soil erodibility factor reflects the ease with which the soil is detached by splash during rainfall or by surface flow, and therefore shows the change in the soil per unit of applied external force of energy. A simpler method to predict *K* was presented by Wischmeier and Smith (1978) that includes the particle size of the soil, organic matter content, soil structure, and profile permeability (Dumas and Printemps, 2010).

The soil erodibility factor (*K*) can be approximated from a nomograph if this information is known (Figure 2). The

RUSLE nomograph estimates erodibility according to Equation (2):

$$K= [2.1\times10^{-4}\times(12-a)\times[Ss\times(100-Sc)]^{1.14}+3.25\times(b-2)+2.5\times(c-3)]/100\times0.1317$$

Where $K$ is the soil erodibility factor (ton ha$^{-1}$ MJ$^{-1}$ mm$^{-1}$), $Ss$ and $Sc$ are the products of the dominant size component and the percentage of the clay, respectively, $a$ is the percent organic matter, $b$ is soil structure code and $c$ is profile permeability class (Ritter and Shirmohammadi, 2000).

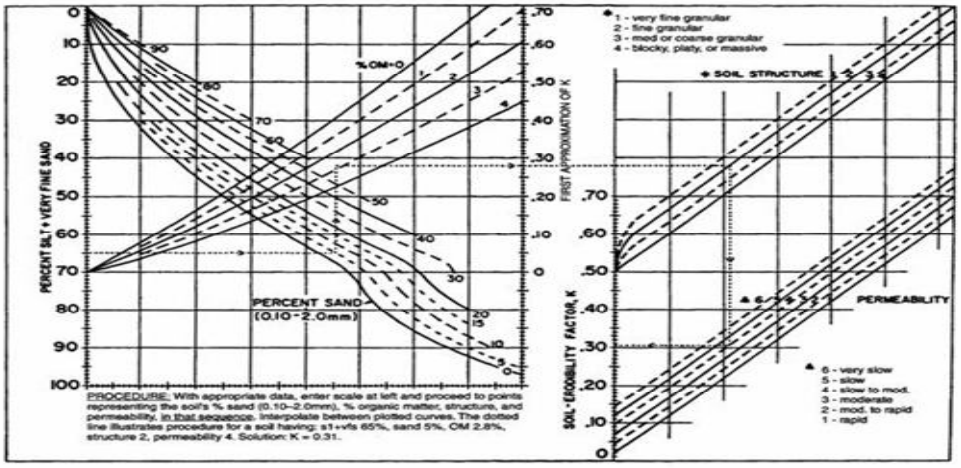


**Figure 2.** The soil erodibility monograph (Wischmeier and Smith, 1987).

**Rainfall erosivity factor (R)**

The rainfall erosivity factor is the product of the kinetic energy contained in rain storms multiplied by their maximum 30-minute intensity for all storms of more than 12.5 mm. Since the values of this factor (intensity of rainfall) are rarely available at standard meteorological stations, mostly monthly and annual mean values of rain are used for estimation of R factor in RUSLE. For assessment of $R$ factor, monthly and annual rainfall were reconstructed for the rainfall stations and the study period. In the next stage, the Fournier index and $R$ factor for all stations were obtained. The Fournier index ($F$) value was obtained from Equation (3) as below (Renard and Freimund, 1994):

$$F = \frac{\sum_{i=1}^{12} p_i^2}{\sum_{i=1}^{12} P}$$

In this equation $P_i$ is the average rainfall in month $i$, and $P$ is the average annual rainfall (mm). Then, using Equations 4 and 5, the Fournier index was calculated for all stations and then with substitution of Fournier index (Equation 3) in the following equations proposed by Renard and Freimund (1994) for the regions lacking detailed data on intensity of rainfall, the $R$ factor value was estimated for the stations.

$$R\text{–factor} = (0.07397 \times F^{1.847})/17.2 \quad \text{If } F < 55 \text{ mm}$$

$$R\text{–factor} = (95.77 - 6.081 \times F + 0.4770 \times F^2)/17.2 \quad \text{If } F > 55 \text{ mm}$$

**Land cover management factor (*C*)**

The *C*-factor is used to express the effect of plants, vegetation canopy and ground cover on annual soil erosion. It is mainly related to the protection of the soil surface by improving water infiltration, intercepting rainfall infiltration and reducing the rainfall energy (Rojas González, 2008; Van der Knijff *et al.*, 2000; Zuazo and Pleguezuelo, 2008; Karaburun, 2010).

Due to the variety of land cover patterns, Remote sensing and GIS techniques have important role in classification and assessment of *C*-factor. Among the several vegetation growth indicators, the Normalized Difference Vegetation Index (*NDVI*) is the most widely used proxy for vegetation cover and production (Panda *et al.*, 2010; Myneni *et al.*, 1997). This index is a numerical indicator that determines the vegetation greenness. *NDVI* is calculated for ETM$^+$ sensor according to Equation (6):

$$NDVI = \frac{NIR - Red}{NIR + Red}$$

Where *NIR*: the spectral reflectance of the near infrared portion and *IR*: the spectral reflectance in the upper visible spectrum. *NDVI* values for each pixel varies from -1.0 to +1.0. A large difference between the two bands results in *NDVI* values at the extremes of the data range. Photosynthetic active vegetation presents a high reflectance in the near *IR* portion of the spectrum (Band 4, Landsat ETM$^+$), in contrast with the visible portion (Red, Band 3, Landsat ETM$^+$); therefore, *NDVI* values for photosynthetically active vegetation will be positive. Areas with low vegetative cover or bare soil, urban areas, as well as inactive vegetation (unhealthy plants) will usually display *NDVI* values fluctuating between -0.1 and +0.1. Clouds and water bodies generate negative or zero *NDVI* values. After production of the *NDVI* image, Equation (7) was used to generate a *C* factor from *NDVI* values (Van der Knijff *et al.*, 2000):

$$C = exp\left[-\alpha \frac{NDVI}{\beta - NDVI}\right]$$

Where $\alpha$ and $\beta$ are unitless parameters that determine the shape of the curve relating to *NDVI* and *C* factor. Van der Knijff *et al.* (2000) found that this scaling approach gave better results than assuming a linear relationship. Finally, the values of 2 and 1 were selected for the parameters of $\alpha$ and $\beta$, respectively.

**Slope length and Steepness factor (LS)**

The topographic factor represents a ratio of soil loss under given condition to that of a site with the "standard" slope steepness of 9% and slope length of 22.6 m. The topographical factor uses two factors which are slope length (*L*) and slope steepness (*S*) (Ganasri and Ramesh, 2016). The slope length factor is defined as the distance from the source of runoff to the point where either deposition begins or runoff enters a well-defined channel that may be part of a drainage network. On the other hand, the steepness factor reflects the influence of slope steepness on erosion (Wischmeier and Smith, 1978). As already pointed out, the longer the slope length the greater the amount of cumulative runoff, and the steeper the slope of the land the higher the velocities of the runoff which contribute to erosion (Jain *et al.*, 2010).

Liu *et al.* (2000) reported that with an increase in the slope steepness from 20 to 40 and 60%, the slope length exponent did not change. Therefore, in the present study, separate equations as given in the USLE for slope gradient < 21% according to Equation (8), and for areas with a slope gradient > 21% were incorporated in the RUSLE according to Equation (9) (Renard *et al.*, 1997).

$$LS = (L/22.13)^m \times (65.41 \times \sin^2\theta + 4.56 \times \sin\theta + 0.065)$$

$$LS = (L/22.1)^{0.7} \times [6.432 \times \sin(\theta^{0.79}) \times \cos\theta]$$

Where *L* is the slope length in *m*, $\theta$ is angle of the slope in degrees, and *m* is an exponent that depends on slope steepness (0.5 for slopes< 5%, 0.4 for slopes ≤ 4% and 0.3 for slopes ≤ 3%) in Equation (8).

**Support practice (P)**

Factor P is used to reflect the effect of land management such as terracing, counter tillage, and permanent barriers or strips that reduce erosion by their influence on drainage patterns, runoff concentration and runoff velocity (Angima *et al.*, 2003; Hyeon and Pierre, 2006). The value of P factor ranges from 0 to 1, and when the value approaches 0, it indicates good conservation practice while the value approaching 1 indicates poor conservation practice (Ganasri and Ramesh, 2016).

**Results and Discussion**

RUSLE is an empirically based model that is able to estimate average annual soil loss and sediment yield based on spatially distributed input data such as rainfall pattern, soil type, topography, crop system, and management practices in a Geographic Information System environment. After establishing the set of factors, input factors were represented as raster GIS layers in the ArcGIS software. In the next stage, the layers were overlaid and multiplied pixel by pixel, using Equations 1 to 5, to evaluate, and generate maps of soil erosion risk and severity.

## RUSLE Parameter Estimation

### Soil erodibility factor (*K*)

For the present study, K factor was assigned based on geological and soil maps. Then, the *K* value for each soil type was determined according to soil erodibility nomograph as proposed by Wischmeier and Smith (1987) (Figure 2) by considering the organic matter content, permeability class, and soil texture. Soil erodibility values varied from 0.05 to 0.2 t ha $MJ^{-1}$ $mm^{-1}$ for sandy and clay soils in the southern and central parts to 0.35 and 0.65 t ha $MJ^{-1}$ $mm^{-1}$ for the loamy and silt loamy soils in the upper parts of the study area, respectively. The highest amount of the soil erosion is spatially related to the areas which indicate quaternary sediments. The estimated *K* values for the textural groups are presented in Table 3 and Figure 3.

**Table 3.** Soil characteristics associated with *K* values.

| Soil type | Erodibility | K value range |
|---|---|---|
| Fine textured; high in clay | low | 0.05-0.15 |
| Course textured; sandy | low | 0.05-0.20 |
| Medium textured, loam | moderate | 0.25-0.45 |
| High silt content | high | 0.45-0.65 |

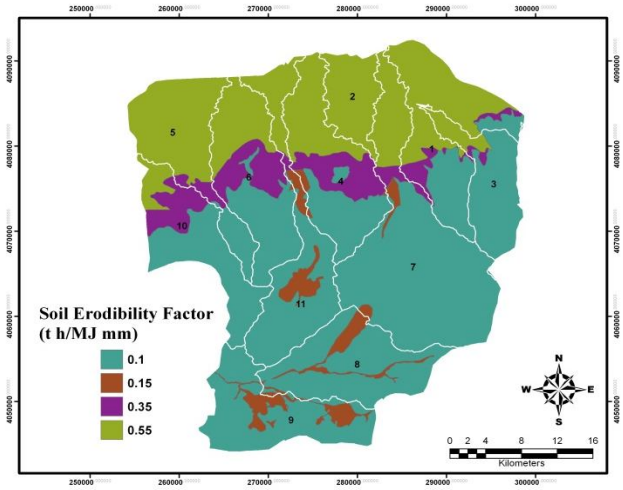


**Figure 3.** The soil erodibility factor (*K*) map of the study area.

### Rainfall erosivity factor (R)

The annual and monthly precipitation data of nine weather stations for 15 years (1999-2014) were used for calculating the Fournier index and R factor using equations (3), (4) and (5). An Inverse Distance Weighted algorithm was used for interpolation of rainfall in the study area. The calculated values for Fournier index and *R* factor are shown in Table 4. The *R*-factor was in the range 4.5 to 240 MJ mm $ha^{-1}$ $h^{-1}yr^{-1}$. The highest *R* values are seen in the southern part of the basin and the lowest occurs in the upper basin (Figure 4).

**Table 4.** Calculation and estimation of *MFI* and *R* for rainfall stations.

| Stations | Longitude | Latitude | Elevation (m) | MFI | R - factor |
|---|---|---|---|---|---|
| Versen | 260589 | 4081379 | 82 | 54 | 6.8 |
| Hashem abad | 272472 | 4081493 | 149 | 43.7 | 4.5 |
| Jalin | 280127 | 4080922 | 135 | 53.4 | 6.69 |
| Jafar abad | 293380 | 4080694 | 245 | 92.9 | 212.5 |
| Nochaman | 258990 | 4072467 | 300 | 98.6 | 240.3 |
| Nahar khoran | 273820 | 4074011 | 569 | 59.7 | 83.3 |
| Shah kooh | 276199 | 4051854 | 2640 | 81.7 | 183.5 |
| Tash | 286714 | 4051353 | 2562 | 69.6 | 142.5 |
| Deh kheyr | 273194 | 4046095 | 2889 | 91.4 | 207.3 |

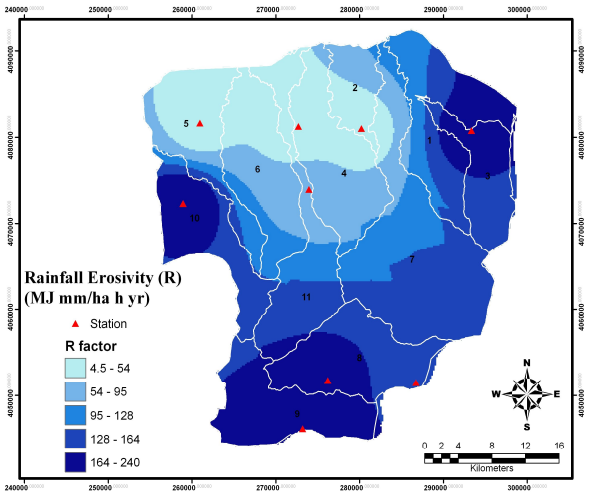


**Figure 4.** Rainfall erosivity factor (*R*) of the study area.

**Cover management factor (*C*)**

In order to determine the *C* factor value for RUSLE, Landsat-ETM$^+$ satellite image was downloaded from earthexplorer site and was used for generating land use parameter in the area. Then, the images were geometrically corrected and ortho-rectified, using Digital Elevation model (DEM) and Ground Control Points (GCPs). In the next stage, training samples were collected for image classification, using field work, and Google Earth. Finally, the maximum likelihood algorithm was implemented for supervised classification of the images. In this process, eight land-use classes were defined. To determine classification accuracy, the map produced by remote sensing analysis was compared with a reference data extracted from different information sources such as Ground Control Points and Google Earth. The achieved overall accuracy and the kappa coefficient were 92.33% and 0.91, respectively (Table 5).

**Table 5.** The classification accuracy of satellite image processing.

| Land use classes | Producer's accuracy | User's accuracy |
|---|---|---|
| Residential area | 90.1 | 100 |
| Dense forest | 100 | 91.66 |
| Semi-dense forest | 100 | 100 |
| Semi-woodland-pasture | 90.9 | 93.02 |
| Thin woodland-pasture | 86.11 | 88.57 |
| Pasture-bare land | 97.5 | 90.69 |
| Agriculture- plantation | 86.2 | 83.33 |
| Bare land | 92.1 | 97.22 |
| Kappa coefficient | 0.91 | |
| Overall accuracy | 92.33 | |

In addition, the *NDVI* map produced from the Landsat–ETM$^+$ satellite image represented values ranging between 0 and 0.73 (Figure 5). Then, the land use map was overlaid with the *NDVI* layer (Figure 6), and the *C* coefficient value for every land use class was assigned (Table 6). As a result, the coefficient of *C* values in the basin varied from 0.004 for the dense forest class to near 1 for the bare land and residential areas. Shit *et al.* (2015) pointed out the model showed logical results after applying the assumed *C* values for each land cover class, with a trend of increasing erosion with low vegetation cover.

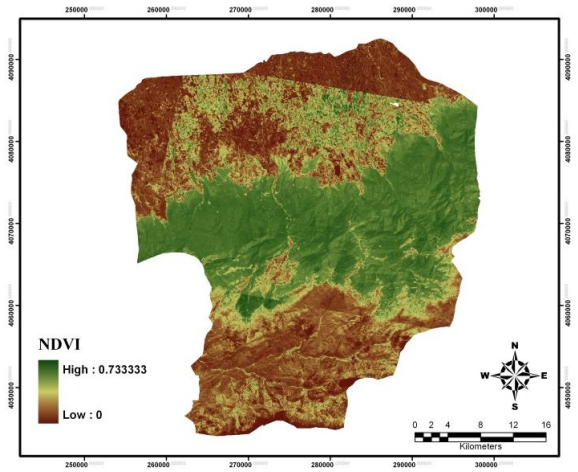


**Figure 5.** NDVI thematic map derived from the Landsat –ETM+ satellite image.

**Table 6.** Average *C* factor values for the several land uses of the study area.

| Land-us/cover | Mean |
|---|---|
| Dense forest | 0.004 |
| Semi-dense forest | 0.025 |
| Pasture-bare land | 0.85 |
| Semi-woodland-pasture | 0.51 |
| Thin woodland-pasture | 0.73 |
| Agriculture- plantation | 0.83 |
| Residential area | 1 |
| Bare land | 0.94 |

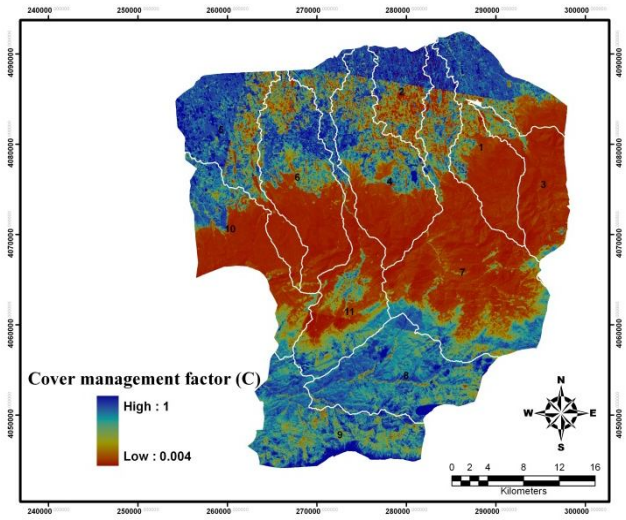


**Figure 6.** Cover management factor (*C*) derived from the NDVI image.

**Slope length and Steepness factor (*LS*)**

The computation of *LS* requires factors such as flow accumulation and slope steepness. The flow accumulation and slope steepness was generated based on DEM layer with a pixel size of 30 meters using Arc hydro extension in ArcGIS software. In the next stage, the sinks in DEM layer were identified using the "sink" tool and were filled using the "Fill" tool. Then, the filled DEM was used as input to calculate the Flow Direction and Flow Accumulation for each cell. Also the steepness was generated in Surface raster tool. In the next stage, the *LS* factor was computed using Raster Calculator in ArcGIS according to Equation

(8). The *LS* factor values in the basin vary from low (0) to high (71). The high *LS* values are related with steep slopes greater than 15°-20° and 20°-30° category in the middle and lower parts of the Gorganrud Basin. The low *LS* factor values consist of mildly rolling hills and flat areas. The combined slope length and steepness map is depicted in Figure 7.

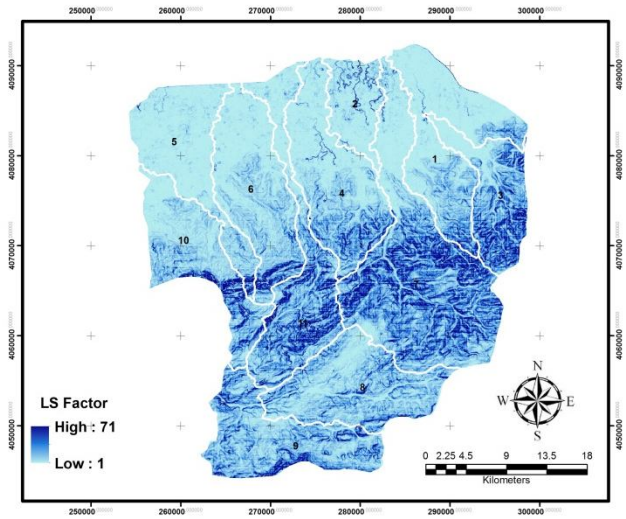


**Figure 7.** Slope length and Steepness factor (*LS*) map of the study area.

**Support practice (*P*)**

As most regions in Gorganrud Basin have but no conservation practice management in place, therefore the *P* factor was defined as 1.0.

**The annual Soil loss**

When all the factors required for the RUSLE were prepared, they were overlaid and soil loss per year was calculated according to the RUSLE equation. Moreover, in order to determine the amount of soil loss from each sub-basin, their boundaries were overlaid with annual soil erosion map. The annual soil loss value for each sub-basin is presented in Figure 8 and Table 7. The annual soil erosion values fluctuate between 0 and 54 t $ha^{-1}$ $yr^{-1}$. The spatial patterns of annual soil loss rates represent that areas with moderate to severe erosion risk (units 1, 2, 3, 4, 5, 6, 9 and 10) are located in the northwest to northeast and eastern parts of the study area, while areas with low erosion to moderate risk (units 7, 8, and 11) are located in the central and southern parts of the study area.

**Table 7.** Minimum, maximum and mean soil loss values for the sub-basins of Gorganrud.

| Sub basins | Min. soil loss (t/ha $year^{-1}$) | Max. soil loss (t/ha $year^{-1}$) | Mean (t/ha $year^{-1}$) | Area ($km^2$) | Area (%) |
|---|---|---|---|---|---|
| 1 | 0 | 31.25 | 19.2 | 30.46 | 2.03 |
| 2 | 0 | 51.05 | 33.6 | 57.55 | 3.8 |
| 3 | 0 | 26.76 | 19.8 | 90.55 | 6.12 |
| 4 | 0 | 31.7 | 21.5 | 146.07 | 9.88 |
| 5 | 0 | 53.6 | 29.3 | 124.25 | 8.42 |
| 6 | 0 | 41.89 | 31.1 | 144.71 | 9.8 |
| 7 | 0 | 26.54 | 10.6 | 280.88 | 19.01 |
| 8 | 0.02 | 22 | 12.5 | 141.85 | 9.6 |
| 9 | 0 | 45.98 | 19.4 | 133.80 | 9.05 |
| 10 | 0 | 54.28 | 27.9 | 32.75 | 2.21 |
| 11 | 0 | 28.61 | 11.6 | 139.24 | 9.41 |

In the next stage, the annual soil erosion map was classified into six risk classes for easy spatial management and hydrological control of soil erosion. The spatial distribution and proportion of soil erosion of the classes are presented in Figure 9. The results in Table 8 show that about 57.5% of the study area is classified under moderate to high erosion risk (>15 tons $h^{-1}$ $y^{-1}$), while the rest of the area (42.5%) is classified as low potential erosion risk. In terms of actual soil erosion risk, the spatial distributions of erosion risk classes were 42.5% as low, 30.33% as moderate, and 27.17% as severe.

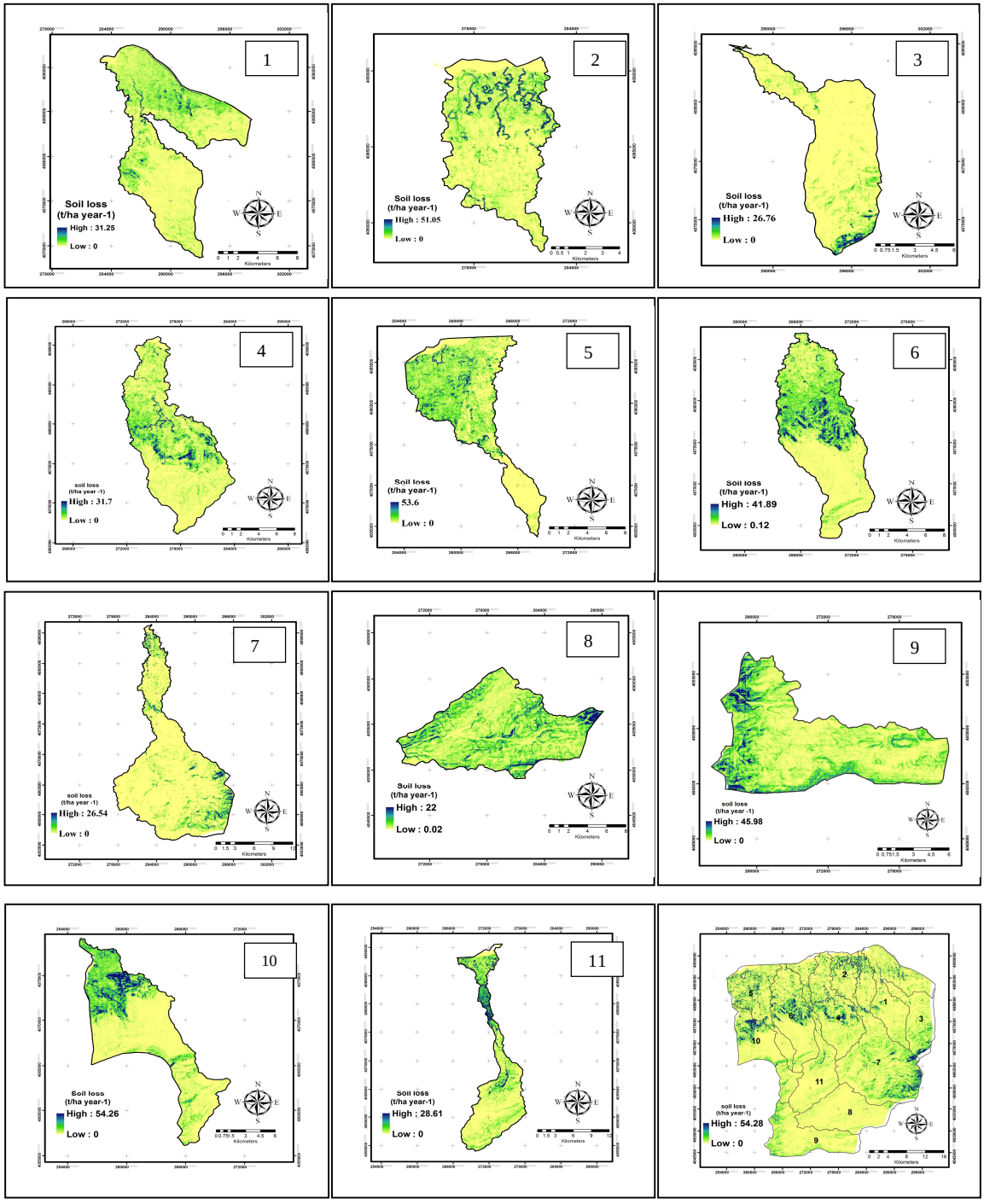


**Figure 8.** Soil loss maps for each sub basin derived from the RUSLE model.

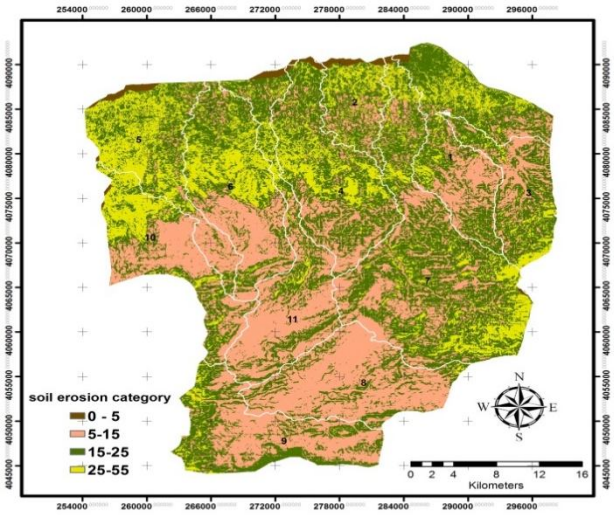


**Figure 9.** The quantitative output of the erosion intensities in the RUSLE model.

**Table 8.** Soil erosion severity zones, their erosion rate and area covered.

| Erosion and torrent category | Erosion intensity category | Rate of soil loss (t/ha $yr^{-1}$) | Area ($Km^2$) | Area (%) |
|---|---|---|---|---|
| I | Very low | 0-5 | 5.3 | 0.41 |
| II | Low | 5-15 | 556.67 | 42.09 |
| III | Moderate | 15-25 | 400.88 | 30.33 |
| IV | Severe | 25-55 | 359.26 | 27.17 |

In order to assess the role of different human activities and vegetation density in the soil erodibility in the sub-basins, the land use map was overlaid with classified soil erosion intensity map. In this way, we found that pastures, plantations, and farmlands comprise the moderate to severe erosion intensities. Population growth, overexploitation, over-cultivation, urbanization, and expansion of economic activities have led to exorbitant removal of vegetation cover. Galdavi *et al.* (2013) pointed out that the prominent changes were occurred in forest land across the basin between 1988 and 2007. Among these changes, a high increase of cultivated lands is coincided with high population growth rates. Therefore, the forest areas around the settlements and agriculture land have been removed completely.

It is postulated elsewhere that the RUSLE parameters can be altered significantly by human activities (Mhangara *et al.*, 2012). The C and P factors can be improved through implementation of environmental practices and vegetation management such as strip cropping, perennial plant cultivation, contour planting, afforestation and use of vegetative filter strips. The LS factor also can be modified by construction of stone contour walls and earthen or stone terraces parallel the contour to stabilize the soil structure against soil erosion. Also, it is appropriate to plant trees on steeper slopes, and on moderate and slightly steep slopes to protect soil from the energy of the raindrops and control soil erosion. The expected benefits of identifying areas susceptible to soil erosion and assigning management and conservation strategies in the studied area could be summarized in the following: control of soil detachment, reduction in sediment delivery ratio to reservoirs, and reduction in runoff peak. The results of soil erosion risk provide a basis for decision makers to compare, rank, and prioritize areas for implementation of conservation and land management plans.

## Conclusion

A quantitative and qualitative assessment of the erosion risk for the soils of Gorganrud Basin was undertaken applying RUSLE equation based on spatially distributed input such as rainfall erosivity, soil

erodibility, slope length and steepness, cover management, and support practice. In the studied basin, the intersect analysis of land use and soil erosion intensity maps indicates that areas with natural forest cover have positive effects on minimum rate of soil erosion, while areas under heavy human influence show opposite effects on rates of soil erosion. By reviewing the value of the criteria maps of the study area, we noted that the slope is not linearly related to the amount of erosion and other factors affected the rate of erosion. In this study, land use and soil factors were more influential than the slope factor. The highest amount of erosion occurred in the northwest to northeast and eastern regions with lithological units including loess, young terraces and alluvial deposits and agricultural use (despite the fact that LS factors have values less than 10). In the central and southern parts of the basin, in spite of high values of LS factor (15–55), the areas depicted low to moderate erosion potential. This is due to the dense forest coverage in the region that decreases the energy of rain droplets. The soil erosion prediction and soil erosion intensity assessment can be helpful for different management practices and sustainable land use prescription for the basin. Areas with a high and increasing risk of erosion are in priority for the implementation of erosion control practices.

**Acknowledgements**

We would like to thank Meysam Mottaki for the scientific discussions and suggestions. We are also grateful to members of the Department of Environmental Science of Gorgan University for their help in collecting the required data.

**References**

Angima, S.D., Stott, D.E., Oneill, M.K., Ong, C.K., and Weesies, G.A. 2003. Soil erosion prediction using RUSLE for central Kenyan highland conditions. Journal of Agriculture, Ecosystem & Environment. 97 (1), 295-308.

Arriaga, F., and Lowery, B. 2003. Erosion and productivity. Encyclopedia of water science. New York, Marcel Dekker.1, 222-224.

Devatha, C.P., Deshpande, V., and Renukaprasad, M.S. 2015. Estimation of soil loss using USLE model for Kulhan Watershed, Chattisgarh. Journal of Aquatic Procedia. 4(2015), 1429-1436.

Dorren, L., Bazzoffi, P., Sánchez Díaz, J., Arnoldussen, A., Barberis, R., Berényi Üveges, J., and *et al.* 2004. Working Group on Soil Erosion Task Group III on Impacts of soil erosion. European commission directorate- general environment. Multi-stakeholder Working Group Reports Soil Thematic Strategy. p. 1-20.

Dumas, P., and Printemps, J. 2010. Assessment of soil erosion using USLE model and GIS for integrated watershed and coastal zone management in the South Pacific Islands. In Proceedings Interpraevent, International Symposium in Pacific Rim, Taipei, Taiwan. Pp: 856-866.

Farhan, Y., Zregat, D., and Farhan, E. 2013. Spatial estimation of soil erosion risk using RUSLE approach, RS and GIS techniques: A case study of Kufranja watershed, northern Jordan. Journal of Water Resource and Protection. 5 (12), 1247-1261.

Galdavi, S., Mohammadzade, M., Salman Mahiny, A., Nejafi Nejad, A. 2013. Forest Change Modeling Using Logistic Regression in the period of 1988- 2007. Journal of Geographic space. 14(46), 51-70.

Ganasri, B.P., and Ramesh, H. 2016. Assessment of soil erosion by RUSLE model using remote sensing and GIS: A case study of Nethravathi Basin. Journal of Geoscience Frontiers. 7(6), 953-961.

Hyeon, S.K., and Pierre, Y.J. 2006. Soil erosion modeling using RUSLE and GIS on the IMHA watershed. Journal of Water Engineering Research. 7 (1), 29-41.

Jain, M.K., Mishra, S.K., and Shah, R.B. 2010. Estimation of sediment yield and areas vulnerable to soil erosion and deposition in a Himalayan watershed using GIS. Journal of Current Science. 98(2), 213-221.

Karaburun, A. 2010. Estimation of C Factor for Soil Erosion Modeling Using NDVI in Buyukcekmece Watershed. Ozean Journal of Applied Sciences. 3 (1), 77-85.

Kheyrodin, H. 2016. Modeling soil erosion in Iran. Innovate International Journal of Medical & Pharmaceutical Sciences. 1(1), 12-16

Kouli, M., Soupios, P., and Vallianatos, F. 2009. Soil erosion prediction using the revised universal soil loss equation (RUSLE) in a GIS framework, Chania, Northwestern Crete, Greece. Journal of Environmental Geology. 57(3), 483-497.

Li, Z.G., and Luo, Z.D. 2006. On method for evaluating soil erosion severity in country scale-index of soil erosion severity and its application. Journal of Bull Soil Water Conservation. 26: 41-51.

Liu, B.Y., Nearing, M.A., Shi, P.J., and Jia, Z.W. 2000. Slope length effects on soil loss for steep slopes. Journal of Soil Science Society of America. 64(5), 1759–1763.

Mhangara, P., Kakembo, V., and Lim, K. 2012. Soil Erosion Risk Assessment of the Keiskamma Catchment, South Africa Using GIS and Remote Sensing. Environmental Earth Science. 65(7), 2087-2102.

Myneni, R.B., Keeling, C.D., Tucker, C.J., Asrar, G., and Nemani, R.R. 1997. Increased plant growth in the northern high latitudes from 1981 to 1991. Journal of Nature. 386(6626), 698–702.

Panda, S.S., Ames, D.P., and Panigrahi, S. 2010. Application of vegetation indices for agricultural crop yield prediction using neural network techniques. Journal of Remote Sens. 2(3), 673–696.

Panagos, P., Borrelli, P., Poesen, J., Ballabio, C., Lugato, E., Meusburger, K., Montanarella, L. and Alewell, C. 2015. The new assessment of soil loss by water erosion in Europe. Environmental Science & Policy, 54, 438-447.

Pathaka, P., Sahrawat, K.L., Rego, T.J., and Wani, S.P. 2005. Measurable biophysical indicators for impact assessment: changes in soil quality. Natural resource management in agriculture: Methods for assessing economic and environmental impacts, 53-74.

Ranzi, R., Le, T.H., and Rulli, M.C. 2012. A RUSLE approach to model suspended sediment load in the Lo river (Vietnam): Effects of reservoirs and land use changes. Journal of Hydrology. 422–423, 17–29.

Renard, K.G., Foster, G.R., Weesies, G.A., McCool, D.K., and Yoder, D.C. 1997. Prediction soil erosion by water: a guide to conservation planning with the Revised Universal Soil Loss Equation. Agricultural handbook No. 703. US Government Printing Office. Washington, DC.

Renard, K.G., and Freimund, J.R. 1994. Using monthly precipitation data to estimate the R factor in the revised USLE. Journal of Hydrology. 157(1-4), 287-306.

Ritter, W.F., and Shirmohammadi, A. 2000. Agricultural nonpoint source pollution: watershed management and hydrology: CRC Press.

Rojas González, A.M. 2008. Soil erosion calculation using RS and GIS in Río Grande De Arecibo watershed, Puerto Rico. Proceedings ASPRS 2008 Annual Conference Bridging the Horizons: New frontiers in geospatial collaboration, Portland, Oregon. April 28th–May 2nd.

Safamanesh, R., Sulaiman, W.N.A., and Ramli, M.F. 2006. Erosion risk assessment using an empirical model of pacific south west inter agency committee method for Zargeh watershed, Iran. Journal of Spatial Hydrology. 6(2), 105-120.

Saha, S.K. 2003. Water and wind induced soil erosion assessment and monitoring using remote sensing and GIS. In: Satellite Remote Sensing and GIS Applications in Agricultural Meteorology. Proceedings of the training workshop, 7-11 July, 2003, Dehra Dun, India. 315-330.

Shit, P.K., Nandi, A.S., and Bhunia, G.S. 2015. Soil erosion risk mapping using RUSLE model on Jhargram sub-division at West Bengal in India. Modeling Earth Systems and Environment. 1(3), 28-40.

The management and planning organization, 2007. Office of Maps and Spatial Information in Golestan Province. Iran.

UNDP. 1999. Human Development Report of Islamic Republic of Iran. Chapter 8. p.109-121.

Van der Knijff, J.M., Jones, R., and Montanarella, L. 2000. Soil erosion risk assessment in Europe. EUR 19044 EN. Office for official publication of the European Soil Bureau. 38pp.

Wischmeier, W.H., and Smith, D.D. 1978. Prediction rainfall erosion losses: a guide to conservation planning. Agriculture handbook No. 537. US Department of Agriculture Science and Education Administration, Washington, DC, USA, 163 pp.

Zuazo, V.H.D., and Pleguezuelo, C.R.R. 2008. Soil-erosion and runoff prevention by plant covers. A review. Agronomy for sustainable development. 28(1), 65-86.